

# Spatiotemporal coherent control of light through a multiply scattering medium with the Multi-Spectral Transmission Matrix

Mickael Mounaix,<sup>1,\*</sup> Daria Andreoli,<sup>1,2</sup> Hugo Defienne,<sup>1</sup> Giorgio Volpe,<sup>1,3</sup> Ori Katz,<sup>1,2</sup> Samuel Grésillon,<sup>2</sup> and Sylvain Gigan<sup>1</sup>

<sup>1</sup>*Laboratoire Kastler Brossel, ENS-PSL Research University, CNRS,*

*UPMC Paris Sorbonne, Collège de France, 24 rue Lhomond, 75005 Paris, France*

<sup>2</sup>*ESPCI ParisTech, PSL Research University, CNRS, Institut Langevin, 1 rue Jussieu, F-75005 Paris, France*

<sup>3</sup>*Department of Chemistry, University College London, 20 Gordon Street, London WC1H 0AJ, UK*

We report broadband characterization of the propagation of light through a multiply scattering medium by means of its Multi-Spectral Transmission Matrix. Using a single spatial light modulator, our approach enables the full control of both spatial and spectral properties of an ultrashort pulse transmitted through the medium. We demonstrate spatiotemporal focusing of the pulse at any arbitrary position and time with any desired spectral shape. Our approach opens new perspectives for fundamental studies of light-matter interaction in disordered media, and has potential applications in sensing, coherent control and imaging.

Propagation of coherent light through a scattering medium produces a speckle pattern at the output [1], due to light scrambling by multiple scattering events [2]. The phase and amplitude information of the light are spatially mixed, thus limiting resolution, depth and contrast of most optical imaging techniques. Ultrashort pulses, generated by broadband mode-locked lasers, are very useful for multiphotonic imaging and non-linear physics [3–5]. In the temporal domain, an ultrashort pulse is temporally broadened during propagation in a scattering medium, due to the long dwell time within it [6, 7], which therefore limits its range of applications.

However, this scattering process is linear and deterministic. Therefore, one can control the input wavefront to design the output field. In this respect, spatial light modulators (SLMs) offer more than a million degrees of freedom to control the propagation of coherent light. These systems have played an important role in the development of wavefront shaping techniques to manipulate light in complex media. Iterative optimization algorithm [8–10] and phase conjugation methods [11, 12] have been proposed to focus light at a given output position, an essential ingredient for imaging. An alternative method for light control is the optical transmission matrix (TM). The TM is a linear operator that links the input field (SLM) to the output field (CCD camera) [13, 14]. The measurement of the TM allows imaging through [15] or inside a scattering medium [16], and potentially access mesoscopic properties of the system [17].

The possibility of shaping the pulse in time is also essential for coherent control [18]. Temporally, photons exit a scattering medium at different times, giving rise to a broadened pulse at its output [7, 19]. Temporal spreading of the original pulse is characterized by a confinement time  $\tau_m$  [20] related to the Thouless time [21]. Equivalently, from a spectral point of view, the scattering medium responds differently for distinct spectral components of an ultrashort pulse, with a spectral correlation bandwidth  $\Delta\omega_m \propto 1/\tau_m$ , giving rise to a very complex spatio-temporal speckle pattern [22–25]. With a single SLM, one can manipulate spatial degrees of freedom to adjust the delay between different optical paths. Therefore spatial and temporal distortions can be both compensated using

wavefront shaping techniques. This approach allows for the temporal compression of an ultrashort pulse at a given position by iterative optimization using as feedback an heterodyne detection [26] or a two-photon absorption signal [27], or alternatively using digital phase conjugation [28]. Another technique consists in shaping only the spectral profile of the pulse at the input, to compensate the temporal distortion induced by the medium [29]. Equivalently to a spectral approach, the measurement of a time-resolved reflection matrix [30, 31] enables light delivery at a given depth of the scattering medium.

Recently, the measurement of a TM of the medium for several wavelengths, the Multi-Spectral Transmission Matrix (MSTM) [22], allowed for both spatial and spectral control at any position in space using a single SLM. In [22], since the spectral phase relation between different matrices was unknown, deterministic temporal control was still elusive. Here, we introduce the MSTM formalism including the spectral phase relation between the different frequency responses of the medium. This additional information gives access to a full spatio-temporal control of an ultrashort pulse propagating in the disordered medium. We demonstrate deterministic spatiotemporal focusing and enhanced excitation of a non-linear process, as well as the deterministic achievement of a variety of temporal profiles.

First, we need to describe the propagation of an ultrashort pulse through the scattering medium, i.e. measure the MSTM. The ratio between the spectral bandwidth of the ultrashort pulse  $\Delta\omega_L$  and  $\Delta\omega_m$  gives the number of independent spectral degrees of freedom  $N_\omega$ . It corresponds to the number of monochromatic TM that one needs to measure to completely describe both spatially and spectrally the propagation of the broadband signal. In [22], the reference signal in the measurement of the MSTM was a co-propagative speckle, as in [14]. Since this reference speckle is also  $\lambda$ -dependent, the spectral phase remained undetermined. Nonetheless, the manipulation of the input field with this incomplete MSTM allows using the scattering medium as a very complex optical component, such as a lens or a grating [22]. Achieving full control of the pulse in the time domain requires the knowledge of the relative phase relation between the wavelengths of the pulse at

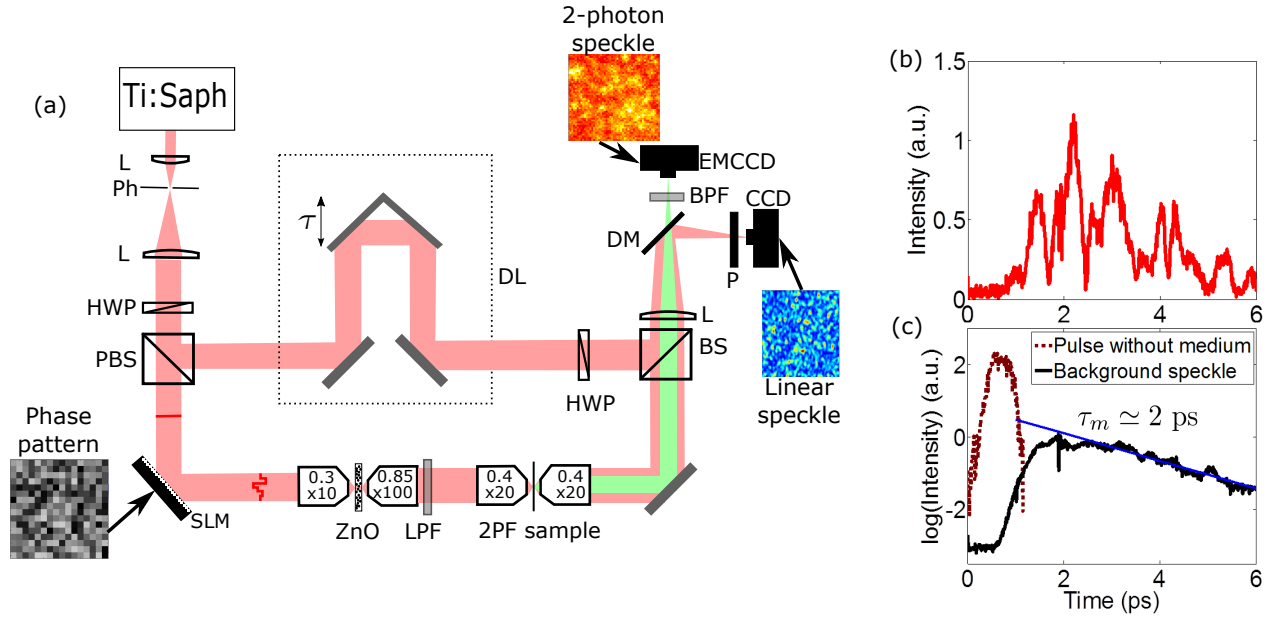


FIG. 1. (Color online) Principle of the experiment. (a) Experimental setup. The laser (ultrashort pulse 110 fs at FWHM) is expanded and illuminates the SLM which is conjugated with the back focal plane of a microscope objective. The scattering medium is a thick (around 100  $\mu\text{m}$ ) sample of ZnO nanoparticles, placed between two microscope objectives. The output plane is imaged on the two-photon fluorescence (2PF) sample. The long-pass filter (LPF) allows one to eliminate the autofluorescence of the ZnO. A dichroic mirror (DM) separates the two-photon fluorescence signal (imaged with an EMCCD) from the linear signal (imaged with a CCD). Lens (L), pinhole (Ph), half plate wave (HPW), polarized beam-splitter (PBS), delay line (DL), beam splitter (BS), polarizer (P), band pass filter (BPF). (b) Temporal speckle from a single spatial speckle grain, obtained with an Interferometric Cross-Correlation (ICC) measurement. (c) ICC of the original pulse in the sample arm without the medium (dotted line), characterized by a time-width of 520 fs at FWHM. ICC of the transmitted pulse through the medium, averaged over 100 different spatial positions of the speckle (solid line), characterized by a decay time of  $\approx 2$  ps (blue line).

the output of the medium. Here, an external reference arm is added to the experimental setup and used as a common reference during a phase stepping holographic process. This technique allows measuring the phase information for each wavelength of the ultrashort pulse in every spatial position at the output. The output field reads:

$$E_j^{\text{out}} = \sum_{i=1}^{N_{\text{SLM}}} \sum_{k=1}^{N_{\omega}} h_{jik} e^{i\varphi_{jk}} E_i^{\text{in}}(\lambda_k) \quad (1)$$

where  $E_j^{\text{out}}$  represents the value of the output field at the  $j$ -th pixel of the CCD camera,  $E_i^{\text{in}}(\lambda_k)$  the value of the input field at the  $i$ -th SLM pixel at wavelength  $\lambda_k$ ,  $h_{jik} e^{i\varphi_{jk}}$  the coefficients of the MSTM with  $\varphi_{jk}$  the spectral phase component.

Fig. 1 illustrates the experimental setup. A Ti:Saph laser source (MaiTai, Spectra Physics) produces a 110fs ultrashort pulse, centered at 800nm with a spectral bandwidth of 10 nm FWHM. The same laser can also be used as a tunable monochromatic laser in the same spectral range. The phase-only SLM (LCOS-SLM, Hamamatsu X10468) is used in reflexion, subdivided in  $32 \times 32$  macropixels. The scattering medium is a thick layer of ZnO nanoparticles randomly distributed on a glass slide, placed between two microscope ob-

jectives. Most experiments are performed on an approximately 100  $\mu\text{m}$  thick sample, characterized by its spectral correlation bandwidth  $\Delta\lambda_m \approx 0.5$  nm (measurement done in the same way than [22]), equivalent to  $\Delta\omega_m \approx 3$  THz. The two paths have the same optical length: when the laser is generating an ultrashort pulse, both the ultrashort reference pulse and the stretched one are overlapped in space and time. The output plane of the scattering medium is imaged on a two-photon fluorescent sample, which is a powder of fluorescein diluted in ethanol, inside a glass capillary (CM Scientific, 20  $\mu\text{m} \times 200 \mu\text{m} \times 5$  cm). The excitation of this non-linear process will be used to differentiate the spatiotemporal from the spatial focusing. A longpass filter is placed between the two sets of microscope objectives to eliminate some residual autofluorescence of the scattering medium. A CCD camera records the linear output intensity, and is used to measure the MSTM. The 2-photon signal is recorded with an EMCCD camera, placed after a dichroic mirror to separate the linear signal from the fluorescence. In a first step, the laser is set to CW, and we measured the MSTM for  $N_{\omega} = 21$  wavelengths in a 13-nm spectral window centered at 800 nm. In essence, for each wavelength, we display a series of phase patterns on the SLM, and for each input pattern, phase stepping holography with the external reference arm wave permits to recover the complex output field. The MSTM is deduced from this set of

measurement. Once the MSTM has been measured, the laser is set back to pulsed operation. The CCD camera integrates the output speckle over time and only recovers its spatial fluctuations. The temporal shape of the speckle is retrieved with an Interferometric Cross-Correlation (ICC) measurement between the stretched pulse and an ultrashort reference by scanning the reference arm. The temporal envelope of this signal is then retrieved by applying a low pass filter in the Fourier domain [32].

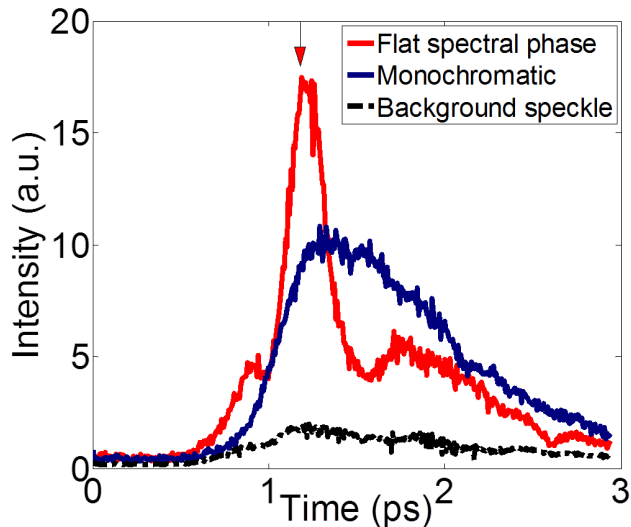


FIG. 2. (Color online) Spatio-temporal focusing with MSTM, averaged over 9 different spatial positions at the output. Spatio-temporal focusing is achieved by imposing a flat spectral phase at the output, whereas spatial focusing is obtained by focusing only the central wavelength of the pulse. The MSTM was measured at a delay-line position corresponding to the top arrow.

The temporal envelope of an output signal recorded at one given spatial position (one speckle grain) is shown on Fig. 1b. The measured output pulse is strongly elongated compared to the initial signal and it shows a very complex temporal structure. Averaging over 100 different output positions allows to recover a smooth shape (Fig. 1c). Its linear decay rate gives access to the confinement time  $\tau_m \simeq 2$  ps corresponding to the time of flight distribution of the photons inside the medium. The value obtained is in agreement with the spectral correlation bandwidth  $\Delta\omega_m$  independently measured. This averaged envelope can be compared to the envelope of the pulse reconstructed without the scattering medium. The ultrashort pulse in the reference arm is transform limited at 110 fs, whereas the same pulse after propagation in the sample arm is dispersed to a time-width of 520 fs at FWHM (mainly because of the microscope objectives).

At this stage, we want to use the MSTM to generate a particular temporal profile at a given output spatial position. The input pattern to focus a given wavelength  $\lambda_k$  at a given position can be simply obtained by phase-conjugating the corresponding line of the monochromatic  $\text{TM}(\lambda_k)$  [14], thus gen-

erating a focus without any temporal compression. To extend this idea to the temporal domain, we can generalize this principle. It is possible, using a single SLM pattern, to focus multiple wavelengths simultaneously at a given position, with a well-defined spectral phase. The corresponding solution can be obtained by algebraically summing all the individual patterns. Since the SLM is phase only, the phase-pattern to display is simply the phase of the solution.

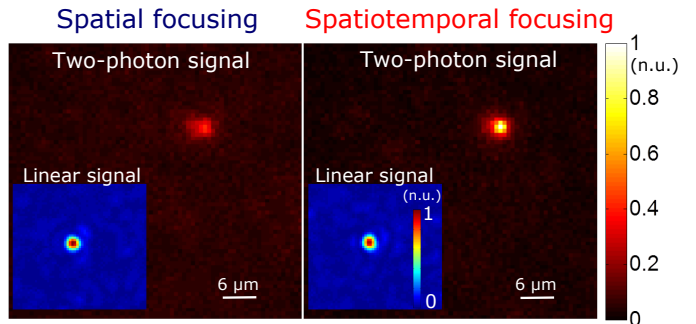


FIG. 3. (Color online) Comparison of 2-photon excitation for spatial and spatiotemporal focusing, obtained with a thinner scattering sample of ZnO ( $\tau_m \simeq 500$  fs). Inset : corresponding CCD signal. Integration time identical for both excitations : 2s for the 2-photon and 1ms for the linear. Scale bars normalized to the maximum intensity of spatiotemporal focusing. We observe a two-fold enhancement of the non-linear signal for the same average intensity when performing spatiotemporal focusing.

The main result is presented in Fig. 2, where we demonstrate temporal compression of the pulse. The presented temporal profiles are retrieved with an ICC measurement. All data are averaged over 9 different spatial positions at the output for better visibility. Imposing a flat spectral phase (i.e. the same spectral phase for all wavelengths) at a chosen spatial position at the output, we observe spatiotemporal focusing at a time determined by the delay line position where the MSTM was previously measured, corresponding to the top arrow in Fig. 2. Temporal compression of the output pulse is obtained almost to its Fourier limited time-width (120 fs at FWHM). The shape of the pulse around the peak is not due to artifacts but is due to the square spectral window used in the MSTM measurement, giving a cardinal sine form with an expected rebound at 400fs from the arrival time of the pulse. As a comparison, spatial focusing is also demonstrated, by focusing only the central wavelength of the output pulse. The observed intensity is higher than the averaged background speckle because the pulse is spatially focused, but temporal compression is missing.

To unequivocally demonstrate the temporal compression, we complement our linear ICC characterization by a two-photon fluorescence measurement. The total intensity of the two-photon fluorescent signal is proportional to the square of the excitation intensity, and also to the inverse of its time-width [33]. Therefore, with an equivalent spatial focusing, a temporal compression corresponds to a higher two-photon

signal. In Fig. 3, the two-photon signal is recorded for both spatial and spatiotemporal focusing with a thinner scattering sample of ZnO (characterized by a measured  $\Delta\lambda_m \simeq 2$  nm) to increase two-photon signal contrast. The signal over noise ratio of the two-photon signal is two times higher when the light is spatiotemporally focused compared to the case where the light is spatially focused, with a similar linear signal in both cases.

The MSTM gives also access to a more sophisticated spectral shape. The control of this information allows any kind of spectral shape at the output of the scattering medium [34], without any additional measurement. In essence, the scattering medium in conjunction with the spatial light modulator can be used as a pulse shaper. Results of temporal control on the output signal are shown in Fig. 4. In Fig. 4a and Fig. 4b a linear spectral phase relation between the wavelengths of the pulse is imposed, thus advancing or delaying the arrival time of the pulse. By tuning the slope of the imposed spectral phase ramp [34], the ultrashort pulse can be temporally shifted with a controllable delay:

$$\tau = -\frac{\delta\phi \lambda_0^2}{2\pi c \delta\lambda} \quad (2)$$

where  $\delta\phi$  is a phase difference between the first and the last wavelength in a spectral interval  $\delta\lambda$  centered around  $\lambda_0$ , and  $c$  is the speed of light. The predicted arrival time of the pulse is indicated by the top arrows on each plot. The ultrashort pulse is focused in the same output spatial position, but its arrival time is changed. Two other important examples are demonstrated. Firstly, a  $\pi$ -phase step between the two halves of the spectrum induces a pulse with a dip, also called an odd pulse [35, 36], which can be extremely useful for coherent control [37]. The corresponding temporal profile is presented in Fig. 4c. Secondly, a linear superposition of a flat phase pulse and a spectral phase ramp pulse at the same spatial position allows the arrival of two pulses with a controllable delay, allowing pump-probe excitation. As an example, we show in Fig. 4d two pulses separated by  $\Delta t = 513$  fs.

In all these experiments, the efficiency of the focusing, i.e. the signal to background ratio of the obtained spatiotemporal shape relative to the background speckle, is proportional to the number of controllable degrees of freedom, here the number of controlled segments on the SLM [8, 14]. It also depends on the number of different spatial or temporal targets and on the number of spectral degrees of freedom  $N_\omega$  to be controlled [38].

In conclusion, our setup allows us to access both the spatial and spectral phase information of the MSTM, thus using the multiply scattering medium in conjunction with the SLM as a lens and a pulse shaper. It is also conceivable to focus two pulses at two different times at two different spatial positions, or to control the duration of the pulse by adding a quadratic phase relation between the frequencies. As these examples indicate, any temporal shape is achievable, with a resolution given by the temporal duration of the pulse,

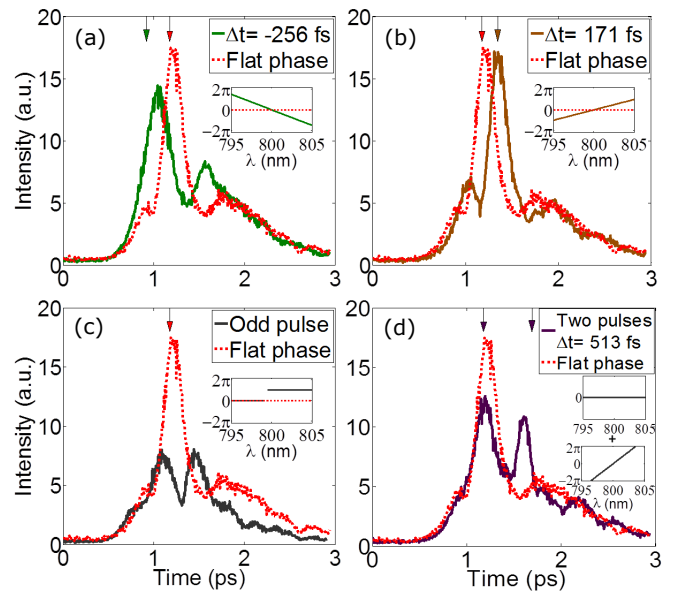


FIG. 4. (Color online) Any suitable spectral shape can be obtained. (a) A negative spectral phase ramp advances the arrival time of the pulse. (b) A positive spectral phase ramp delays the pulse. (c) A  $\pi$ -phase step in the spectral domain creates an odd pulse. (d) The sum of a flat phase pulse and a spectral phase ramp pulse gives two pulses with a controlled delay at the same output spatial position. Inset : spectral phase profile applied to the signals. Top arrows indicate the expected arrival time of the pulse.

over a temporal interval related to the confinement time of the medium. It can be achieved using only spatial degrees of freedom of a single SLM. This temporal control could enable coherent quantum control [39], or the excitation of localized nano-objects, and open interesting perspectives for the study of light-matter interaction and for non-linear imaging in multiply scattering media.

The authors would like to thank Thomas Chaigne for inspiring discussions. This work was funded by the European Research Council (grant no. 278025)

\* mickael.mounaix@lkb.ens.fr

- [1] JW. Goodman, *JOSA* **66** 1145 (1976).
- [2] P. Sebbah, *Springer Science & Business Media* (2012).
- [3] M. Oheim et al., *Journal of neuroscience methods* **111** 29–37 (2001).
- [4] W. Denk et al., *Science* **248** 73 (1990).
- [5] T. Brabec et al., *Rev. Mod. Phys.* **72** 545 (2000).
- [6] NC. Bruce et al., *Applied optics* **34** 5823 (1995).
- [7] PM. Johnson et al., *Phys. Rev. E* **68** 016604 (2003).
- [8] IM. Vellekoop et al., *Opt. Lett.* **32** 2309–2311 (2007).
- [9] IM. Vellekoop et al., *Phys. Rev. Lett.* **101** 120601 (2008).
- [10] IM. Vellekoop et al., *Optics Communications* **281** 3071 (2008).
- [11] IN. Papadopoulos et al., *Opt. Exp.* **20** 10583 (2012).
- [12] Z. Yaqoob et al., *Nat. Photon.* **2** 110 (2008).
- [13] CWJ. Beenakker, *Rev. Mod. Phys.* **69** 731 (1997).

- [14] S.M. Popoff et al., *Phys. Rev. Lett.* **104** 100601 (2010).
- [15] S.M. Popoff et al., *Nat. Comm.* **1** 81 (2010).
- [16] T. Chaigne et al., *Nat. Photon.* **8** 58 (2014).
- [17] A. Goetschy et al., *Phys. Rev. Lett.* **111** 063901 (2013).
- [18] JMD. Cruz et al., *PNAS* **101** 16996 (2004).
- [19] M. Tomita et al., *JOSA B* **12** 170 (1995).
- [20] N. Curry et al., *Opt. Lett.* **36** 3332–3334 (2011).
- [21] DJ. Thouless, *Physics Reports* **13** 93 (1974).
- [22] D. Andreoli et al., *Sci. Rep.* **5** (2015).
- [23] AP. Mosk et al., *Nat. Photon.* **6** 283–292 (2012).
- [24] E. Small et al., *Opt. Lett.* **37** 3429 (2012).
- [25] F. van Beijnum et al., *Opt. Lett.* **36** 373 (2011).
- [26] J. Aulbach et al., *Phys. Rev. Lett.* **106** 103901 (2011).
- [27] O. Katz et al., *Nat. Photon.* **5** 372 (2011).
- [28] EE. Morales-Delgado et al., *Opt. Exp.* **23** 9109 (2015).
- [29] D. McCabe et al., *Nat. Comm.* **2** 447 (2011).
- [30] Y. Choi et al., *Phys. Rev. Lett.* **111** 243901 (2013).
- [31] S. Kang et al., *Nat. Photon.* **9** 253 (2015).
- [32] A. Monmayrant et al., *Journal of Physics B: Atomic, Molecular and Optical Physics* **43** 103001 (2010).
- [33] WR. Zipfel et al., *Nat. Biotechnol.* **21** 1369 (2003).
- [34] AM. Weiner, *Review of Scientific Instruments* **71** 1929 (2000).
- [35] AM. Weiner et al., *Revue de Physique Appliquée* **22** 1619 (1987).
- [36] AM. Weiner et al., *Quantum Electronics, IEEE Journal of* **28** 908 (1992).
- [37] D. Meshulach et al., *Phys. Rev. A* **60** 1287 (1999).
- [38] F. Lemoult et al., *Phys. Rev. Lett.* **103** 173902 (2009).
- [39] D. Meshulach et al., *Nature* **396** 239 (1998).